

# Predicting the modulation of UV-vis absorption and emission of mono-substituted pyrido[2,3,4-*kl*]acridines by electronic density variations analysis

Martin Tiano\*, Chloé Courdurié, Pauline Colinet

Laboratoire de Chimie, Université de Lyon, ENS de Lyon, CNRS UMR 5182, Université Claude Bernard Lyon 1, F69342 Lyon, France.  
E-mail : martin.tiano@ens-lyon.fr

---

## Abstract

DFT and TD-DFT calculations were performed to rationalize the link between UV-Visible absorption and emission spectra and the nature and position of a substituent on the heteroaromatic pyrido[2,3,4-*kl*]acridine skeleton. By studying the variation of electronic density and atomic partial charges between the ground state and the first excited state, we describe here a quantitative method to predict the modulation of UV-Visible spectroscopic properties depending on the nature and the position of a substituent.

**Keywords:** TD-DFT, Electronic Density, Pyrido[2,3,4-*kl*]acridine, UV-Visible spectroscopy, Hammett parameter

---

## 1. Introduction

Finding the best candidate compounds for a specific application is a long process, that usually needs to synthesize a lot of different products before identifying the good ones. For biological applications, quantitative structure-activity relationship, molecular dynamic simulation or molecular docking are rational methodologies to achieve this goal faster than blind testing.[1, 2] For spectroscopic applications in the UV-visible domain, TD-DFT studies of electronic transitions and the parameters which influence them could play a major role to guide the synthesis of a restricted number of candidates for bio-imaging, optic devices, dyes, etc. Indeed, for more than 20 years TD-DFT was extensively used to simulate the optical properties of organic molecules.[3, 4] Benchmarks and tutorial reviews make easy to select simulation methods with accurate calculations, and great efforts have been made to rationalize the influence of the geometry of molecules, as well as of the charge transfer during the GS-ES1 transition, vibronic couplings, and of the solvent on the UV-vis spectra.[5, 6, 7, 8]

In their experimental and theoretical study of Seoul-Fluor analogs, E. Kim *et al.* have pinpointed that the modulation of the emission wavelength of their compounds is linked to the modifications of HOMO and LUMO energies by adding diverse electron-donor or electron-withdrawing groups on one specific position.[9] Although relatively efficient in their case, this approach did not take into account the whole molecular orbitals implied in the transition between the ground state (GS) and the first excited state (ES1), nor questioned the substitution position.

Focusing on pyrido[2,3,4-*kl*]acridine molecules, we offer here to elaborate on this issue by looking at the electronic density and its variation during GS-ES1 transition for different mono-substituted structures. This would hopefully provide better insights and be more accurate in establishing quantitative relationship between structures and spectroscopic properties.

Pyrido[2,3,4-*kl*]acridine is an aromatic tetracyclic pattern (Figure 1) which is present in almost 100 natural products isolated from sponges or tunicate species. For three decades, numerous studies showed that natural pyrido[2,3,4-*kl*]acridines present very interesting and various biological properties, from cytotoxicity, to antibacterial, antifungal, antiviral, insecticidal, anti-HIV, and anti-parasitic activities. In particular, pyridoacridines can intercalate into DNA double-strands and interfere with topoisomerase-type enzymes. Moreover, some of them have also stronger interactions with guanine quadruplex, and inhibit telomerase complex.[10] Known pyrido[2,3,4-*kl*]acridines are also diversely colored and UV-visible spectra has been reported in the litterature.[11] Some of them are also fluorescent. But, to our knowledge, the only fluorescent spectrum reported to date is the one of kuanoni-amine B, a natural pentacyclic pyrido[2,3,4-*kl*]acridine ( $\lambda_{em} = 524 \text{ nm}$  in methanol)[12, 13] (Figure 1). No other comprehensive spectroscopic study of pyrido[2,3,4-*kl*]acridine structures has been undertaken, despite an intense and productive effort of total synthesis of the natural products members of this family.[14, 15] We think that the combination of these spectroscopic and biological properties makes pyrido[2,3,4-*kl*]acridine derivatives excellent candidates for bio-imaging and theranostic approaches, keeping in mind that the absorbent properties of organic tissues imply the need to tune the luminescent wavelength above 650 nm.[16] In this work, we performed a comprehensive TD-DFT study of UV-Visible absorption and fluorescent emission properties of mono-substituted pyridoacridines. In particular, we found that GS-ES electronic density variations quantitatively correlate with the modulation of the emission and absorption wavelengths in substituted pyrido[2,3,4-*kl*]acridine, allowing us to pre-select excellent candidates for bio-imaging applications.

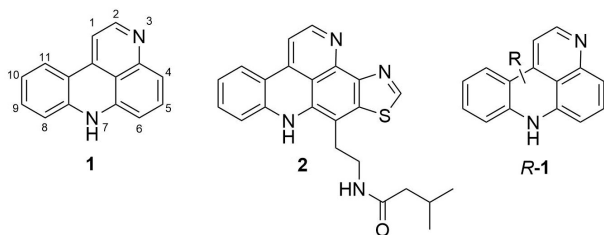


Figure 1: investigated pyrido[2,3,4-*kl*]acridines and typical natural structures. R represents the substituent: for example, **10-Me-1** is the pyrido[2,3,4-*kl*]acridine **1** with a methyl group on position 10.

## 2. Methods

### 2.1. Computational details

All DFT and TD-DFT calculations were performed using the Gaussian 16 program package [17]. The hybrid B3LYP[18, 19, 20], cam-B3LYP[21] or PBE0[22] functionals were used together with 6-31G(d), 6-311+G(d,p) and 6-311++G(d,p) basis sets. Solvent effects were included by using the conductor polarizable continuum model (CPCM) with state-specific corrected linear response (cLR) approach.[23, 24, 25]. The 0-0 transition energies were determined by using the adiabatic Hessian Franck-Condon method implemented in Gaussian 16 package.

### 2.2. Description of the investigated structures

The molecules investigated in this study are pyrido[2,3,4-*kl*]acridine **1**, mono-substituted pyrido[2,3,4-*kl*]acridine bearing methyl (Me) **Me-1**, methoxy (MeO) **MeO-1**, nitrile (CN) **CN-1**, formyl (Oxo) **Oxo-1**, acetyl (Ac) **Ac-1**, fluoro (F) **F-1**, trifluoromethyl (CF<sub>3</sub>) **CF<sub>3</sub>-1**, amino (NH<sub>2</sub>) **NH<sub>2</sub>-1**, methylamino (NHMe) **NHMe-1**, dimethylamino (NMe<sub>2</sub>) **NMe<sub>2</sub>-1**, hydroxyl (OH) group **OH-1** at diverse positions. Chloroform was systematically used as implicit solvent in simulations.

## 3. Results and discussion

### 3.1. Validation of the simulation method

Comparison of experimental and simulated 0-0 transition energy is a relevant manner to check the accuracy of the simulation methods.[26] Although, as no full UV-vis nor fluorescence spectrum of pyrido[2,3,4-*kl*]acridine substrates is available in literature, we first determined the experimental 0-0 transition energy of the unsubstituted pyrido[2,3,4-*kl*]acridine **1** in chloroform ( $E_{exp}^{0-0} = 2.58$  eV, see *Supp. Info.*). We compared that value to the calculated ones by (TD)-DFT with PBE0, B3LYP, cam-B3LYP functionals with different basis set with implicit chloroform (Table 1).

In our case, B3LYP/6-311+G(d,p) and B3LYP/6-311++G(d,p) calculations presented the best agreement with the experimental data. The inclusion of diffuse functions in the basis set improved the results, and the use of 6-311++G(d,p) didn't improve the calculations. Results from PBE0 and cam-B3LYP functional calculations were

Table 1: Simulation parameters optimization with pyrido[2,3,4-*kl*]acridine **1** in chloroform.  $E_{calc}^{0-0}$  are the calculated 0-0 transition energies.  $\Delta E$  is the difference between  $E_{calc}^{0-0}$  and  $E_{exp}^{0-0}$

functional/base	$E_{calc}^{0-0}$ (eV)	$\Delta E$ (eV)
B3LYP/6-31G(d)	2.65	0.07
B3LYP/6-311+G(d,p)	2.57	0.01
B3LYP/6-311++G(d,p)	2.57	0.01
PBE0/6-311+G(d,p)	2.67	0.09
cam-B3LYP/6-311+G(d,p)	2.96	0.38

less consistent with the experimental value, whereas B3LYP provided very good results. However, since the match between modeling and experiment could only be verified on a single substrate, it is difficult to assess the accuracy of this level of theory for the other considered molecules : depending on the nature and the position of the substitution, mono-substituted pyrido[2,3,4-*kl*]acridines could undergo more significant charge transfers during the GS-ES1 transition, which would be mistreated by the B3LYP and PBE0 functionals.[27] We used thus both B3LYP and the range-separated hybrid functional cam-B3LYP, together with the 6-311+G(d,p) basis set. Since we found very similar results with these two functionals, we present here calculations at B3LYP/6-311+G(d,p) level, and all the data with cam-B3LYP/6-311+G(d,p) are also available in the *Supplementary Informations*.

### 3.2. Presentation of the methodology

We started by examining the variation of electronic density between the ground state (GS) and the first excited state (ES1) of the unsubstituted pyrido[2,3,4-*kl*]acridine **1** to identify the spatial distribution and the amplitude of this variation, using the methodology proposed by T. Le Bahers *et al.* (Figure 2).[6]. On a qualitative point of view, positions 4 and 6 of the structure showed the major variation, with an electronic impoverishment. This led us to infer two hypothesis :

- Positions with the larger electronic variations are the more *sensitive* : substituent on that positions should greatly affect the GS-ES1 transition energy.
- For a given position, the nature of the substituent, namely how much electron donor or electron withdrawing group it is, should impact the transition (GS-ES1) energy. If the electronic density increases, an electron withdrawing group would stabilize the excited state, and so decrease the transition energy. On the other hand, if the electronic density decreases, an electron withdrawing group would destabilize the excited state, and so increase the transition energy.

This behaviour would result in a wavelength shift in both absorption and emission spectra of the mono-substituted pyridoacridines compared with the unsubstituted one (**1**).

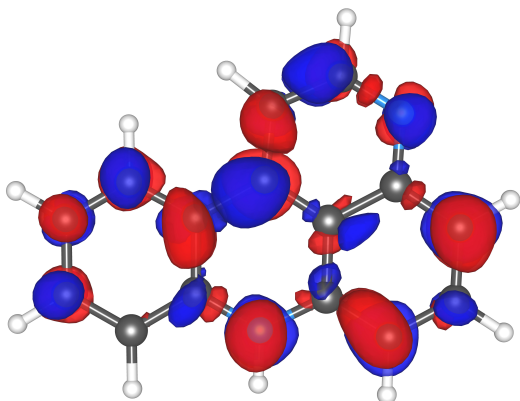


Figure 2: Difference in total electronic density between ground and first excited states computed at B3LYP/6-311+G(d,p) level of theory ( $\Delta\rho(r) = \rho_{EX}(r) - \rho_{GS}(r)$ , isocontour value 0.02 au).

### 3.3. Relationship between the GS-ES partial charge variations at the substituted position and absorption and emission wavelengths

We calculated the variations of the partial atomic charges between the ground state and the first excited state (noted  $\Delta\rho$ ) of each positions of the unsubstituted pyrido[2,3,4-*kl*]acridine, using different charge models (*i.e.* Mulliken, Merz-Kollman, Hirshfeld, CM5, Electrostatic potential charges (ESP) models). We looked at the influence of the substitution site on the variation of the maximum wavelength absorption (resp. emission) for mono-substituted (**1**) compared with (**1**) taken as reference. The variation is noted  $\Delta(\Delta E_{abs})$  (respectively  $\Delta(\Delta E_{em})$ ) (See *Supp. Info.*). We used the methoxy (-OMe), and the methyl groups (-Me) as models of electron donating substituent and the cyano (-CN) group as a model of electron withdrawing substituent (Table 2).

Table 2: Correlation between  $\Delta(\Delta E)$  for MeO and CN substituted pyrido[2,3,4-*kl*]acridine and partial charge variations between GS and ES, depending on partial charge models. In parentheses,  $R^2$  when **2-MeO-1** and **5-MeO-1** (resp. **2-CN-1** and **5-CN-1**) are excluded.

Substituent	Charge model	$R^2$ for abs	$R^2$ for em
MeO	Mulliken	< 0.1	< 0.1
MeO	Merz-Kollman	0.21 (0.76)	0.35 (0.87)
MeO	Hirshfeld	0.66 (0.86)	0.78 (0.89)
MeO	CM5	0.38 (0.85)	0.54 (0.90)
MeO	ESP	0.36 (0.93)	0.52 (0.89)
CN	Mulliken	< 0.1	< 0.1
CN	Merz-Kollman	< 0.1 (0.63)	< 0.1 (0.62)
CN	Hirshfeld	0.77 (0.89)	0.81 (0.96)
CN	CM5	0.54 (0.88)	0.65 (0.95)
CN	ESP	0.63 (0.77)	0.79 (0.84)

Hirshfeld model gave the strongest correlations for both methoxy and cyano substituted structures (Figures 3 and 4). In the case of methyl substituted pyridoacridines, weaker correlations are observed (for example  $R^2 = 0.55$  for  $\Delta(\Delta E_{abs})$  with Hirshfeld charge model), due to the small energy variation between the substituted and the unsubstituted pyrido[2,3,4-

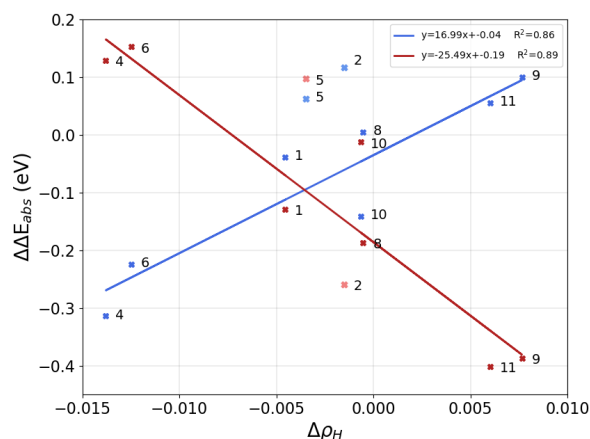


Figure 3: Correlation between  $\Delta(\Delta E_{abs}) = \Delta E_{abs}(\text{\#-MeO-1}) - \Delta E_{abs}(\mathbf{1})$  (blue line) and  $\Delta(\Delta E_{abs}) = \Delta E_{abs}(\text{\#-CN-1}) - \Delta E_{abs}(\mathbf{1})$  (red line) and the partial charge variations between GS and ES of the carbon in position # in compound **1** (Hirshfeld charge model). Line equations and  $R^2$  calculated without positions 2 and 5.

*kl*]acridines (see *Supp. Info.*) We noticed that calculated energies for position 2 and position 5 substituted structures do not fit as well as the other positions. That could be explained by the proximity of the nitrogen and the position 2, and the subsequent interactions between the substituent and the nitrogen lone pair. In the case of the structures substituted in position 5, that could be explained by the relatively small charge variations which occur at position 5.

### 3.4. Relation between Hammett parameter of the substituent and absorption and emission wavelength

We focused on the more *sensitive* positions (*i.e.* positions 4, 6, and 2), and calculate  $\Delta E_{em}$  and  $\Delta E_{abs}$  for different electron donor (EDG) or electron withdrawing groups (EWG). Confirming our intuition and our first results (see *section 3.3*), the substitution of the positions 4 or 6 with an EWG (respectively an EDG) implies an increase (respectively a decrease) of both  $\Delta E_{em}$  and  $\Delta E_{abs}$ , and the opposite results were obtained with position 2.

To quantify this effect, we used  $\sigma_p$  and  $\sigma_m$  Hammett parameters and the Remya parameter  $\Delta V_C$ , as numeric scales for the electron withdrawing or the electron donating strength of the substituents.  $\sigma_p$  and  $\sigma_m$  are empiric parameters determined by kinetic and thermodynamic studies of the influence of the para- or meta-substitution of benzoic acids on their reaction with water.[28]  $\Delta V_C$  parameter is a theoretical parameter derived from molecular electrostatic potential (MESP) analysis of mono-substituted benzene rings, proposed by Remya and Suresh. [29]  $\sigma_p$ ,  $\sigma_m$  and  $\Delta V_C$  parameters are now tabulated for hundreds of chemical groups, and accurately reflect the electron withdrawing or electron donating character of each of them.[29, 30]

We calculated  $\Delta(\Delta E_{em})$  and  $\Delta(\Delta E_{abs})$  for mono-substituted pyrido[2,3,4-*kl*]acridines in position 2 (9 examples), 4 (11 examples) and 6 (10 examples). The best correlations were ob-

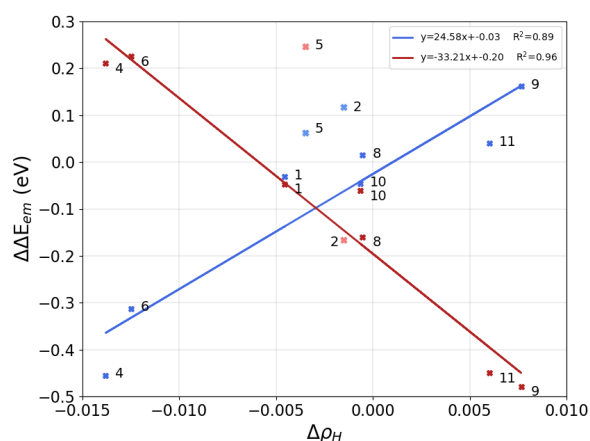


Figure 4: Correlation between  $\Delta(\Delta E_{em}) = \Delta E_{em}(\mathbf{X-MeO-1}) - \Delta E_{em}(\mathbf{1})$  (blue line) and  $\Delta(\Delta E_{em}) = \Delta E_{em}(\mathbf{X-CN-1}) - \Delta E_{em}(\mathbf{1})$  (red line) and the partial charge variations between GS and ES of the carbon in position # in compound **1** (Hirshfeld charge model). # is the position of Methoxy (blue line) and Cyano (red line) substituents. Line equations and  $R^2$  calculated without positions 2 and 5.

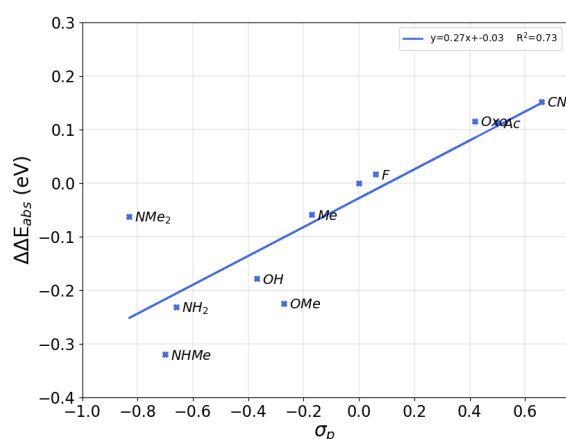


Figure 5: Correlation between  $\Delta(\Delta E_{abs}) = \Delta E_{abs}(\mathbf{6-#-1}) - \Delta E_{abs}(\mathbf{1})$  and the Hammett Parameter  $\sigma_p$  of the substituent #.

tained with  $\sigma_p$  and  $\Delta V_C$  parameters (Figures 5 and 6, and *Supp. Info.*).

For positions 4 and 6,  $\Delta(\Delta E_{abs})$  and  $\Delta(\Delta E_{em})$  clearly correlated linearly with  $\sigma_p$  and  $\Delta V_C$  (Figures 5 and 6, and *Supp. info.*). However, we noticed that  $\Delta(\Delta E_{abs})$  of 6-NMe<sub>2</sub>-**1** was higher than our model predictions. Actually, at the contrary of NH<sub>2</sub> and NHMe substituent, the lone pair of the nitrogen of this group in 6-NMe<sub>2</sub>-**1** is perpendicular to  $\pi$  system, probably involved in an intramolecular hydrogen bond with the N-H in position 7, that makes harder the prediction of the influence of this substituent on transition energies (see Figure S25). It should be also noted that this calculations with cam-B3LYP fonctionnal gave, in this particular structure, a much better consistency between  $\Delta(\Delta E_{abs})$  and  $\sigma_p$  (Figure S17). That could be explained by a stronger charge transfer in 6-NMe<sub>2</sub>-**1** than in the other molecules, that lead to an overestimation of

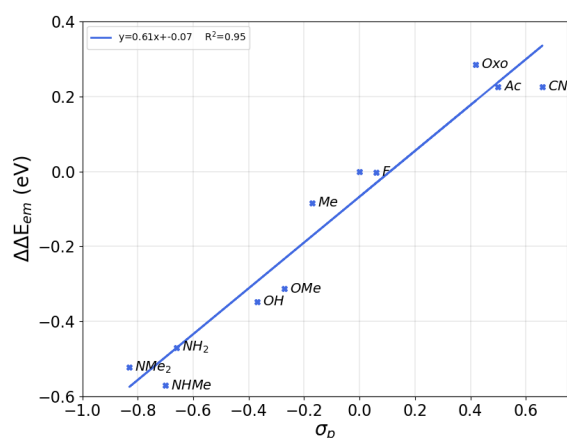


Figure 6: Correlation between  $\Delta(\Delta E_{em}) = \Delta E_{em}(\mathbf{6-#-1}) - \Delta E_{em}(\mathbf{1})$  and the Hammett Parameter  $\sigma_p$  of the substituent #.

it by B3LYP functional : we actually found a charge transfer dipole moment  $\mu_{CT} = 8.573 D$  with B3LYP/6-311+G(d,p), and  $\mu_{CT} = 6.104 D$  with cam-B3LYP/6-311+G(d,p) method, confirming that hypothesis.[6]

The correlations were however weaker ( $R^2 \approx 0,5 - 0,7$ ) for substitutions in position 2 (See *Supp. Info.*). The quite large variations of the transition energy from one to another substituent on that position probably reflect the strong influence of the nitrogen lone pair in position 3.

It is noteworthy that in a study about substituted aryl hydrazones of 1,8-naphthalimide, D. Cheshmedzhieva *et al.* have already highlighted correlations between  $\sigma_p$  and  $\lambda_{fluo}$  for 5 mono-substituted structures, but they noticed that correlation differs in regard to the ED or EW status of the substituent, that they interpreted as a consequence of large charge transfers.[31] In our case, calculated charge transfers are more modest for the studied mono-substituted pyrido[2,3,4-kl]acridines, as evidenced by the evaluation of the parameters  $D_{CT}$  (CT distance) and  $\mu_{CT}$  (see *Supp. Info.*).[6] Thus, as expected, we did not observe any slope breaks between EDG and EWG correlations with  $\sigma_p$  nor  $\Delta V_C$  in our cases.

#### 4. Conclusion

In our attempt to rationalize the effort to tune the UV-Visible spectroscopic properties of pyrido[2,3,4-kl]acridine derivatives, we investigated a simple *in silico* methodology to predict the influence of both the position and the nature of a substituent on the lowest absorption energy and emission energy. Except for one position, the variation of partial charges between the GS and the ES1 of the unsubstituted pyrido[2,3,4-kl]acridine calculated by (TD)-DFT with Hirshfeld model accurately reflected the *sensitivity* of each positions, *i.e.* how much a given substituent on the position change the absorption or emission transition energy. In a second aspect, for a given position on the aromatic core, we showed that the variations of  $\Delta E_{em}$  and  $\Delta E_{abs}$  between the mono-substituted structure and the unsubstituted

one are quantitatively linked to the Hammett parameter  $\sigma_p$  and Remya parameter  $\Delta V_C$ . Thanks to this work, we have identified several candidates with probable near infrared fluorescence for theranostic applications, the synthesis of which are currently underway. We believe that this methodology should be successfully applied on other fluorescent structures, and should save time and energy to find the best adapted candidates for numerous applications, from bio-imaging to organic luminescent devices.

## 5. Author contributions

**Martin Tiano** : Conceptualization, Methodology, Supervision, Investigation, Writing -Original draft-.

**Chloe Courdurie** : Investigation, Writing -Review and editing-, Visualization

**Pauline Colinet** : Validation, Methodology, Visualization, Writing -Original draft-.

## 6. Conflict of Interest

The authors declare no competing financial interest.

## 7. Acknowledgement

The authors acknowledge the SYSPROD project and AXEL-ERA Pôle de Compétitivité for financial support (PSMN Data Center) and Dr. Tangui Le Bahers for very useful discussions.

## References

- [1] G. R. Sliwoski, J. Meiler, E. W. Lowe, *Computational Methods in Drug Discovery*, *Pharmacological Reviews* 66 (1) (2014) 334–95. doi:10.1124/pr.112.007336.
- [2] D. Ramirez, *Computational Methods Applied to Rational Drug Design*, *The Open Medicinal Chemistry Journal* 10 (1) (2016) 7–20. doi:10.2174/1874104501610010007.
- [3] C. Adamo, D. Jacquemin, The calculations of excited-state properties with time-dependent density functional theory, *Chem. Soc. Rev.* 42 (2013) 845–856. doi:10.1039/C2CS35394F. URL <http://dx.doi.org/10.1039/C2CS35394F>
- [4] A. D. Laurent, D. Jacquemin, Td-dft benchmarks: A review, *International Journal of Quantum Chemistry* 113 (17) (2013) 2019–2039. arXiv:<https://onlinelibrary.wiley.com/doi/pdf/10.1002/qua.24438>, doi:<https://doi.org/10.1002/qua.24438>. URL <https://onlinelibrary.wiley.com/doi/abs/10.1002/qua.24438>
- [5] D. Jacquemin, V. Wathelet, E. A. Perpète, C. Adamo, Extensive TD-DFT benchmark: Singlet-excited states of organic molecules, *Journal of Chemical Theory and Computation* 5 (9) (2009) 2420–2435. doi:10.1021/ct900298e.
- [6] T. Le Bahers, C. Adamo, I. Ciofini, A qualitative index of spatial extent in charge-transfer excitations, *Journal of Chemical Theory and Computation* 7 (8) (2011) 2498–2506. doi:10.1021/ct200308m.
- [7] D. Jacquemin, E. Brémond, A. Planchat, I. Ciofini, C. Adamo, Td-dft vibronic couplings in anthraquinones: From basis set and functional benchmarks to applications for industrial dyes, *Journal of Chemical Theory and Computation* 7 (6) (2011) 1882–1892, pMID: 26596449. arXiv:<https://doi.org/10.1021/ct200259k>, doi:10.1021/ct200259k. URL <https://doi.org/10.1021/ct200259k>
- [8] A. Charaf-Eddin, A. Planchat, B. Mennucci, C. Adamo, D. Jacquemin, Choosing a functional for computing absorption and fluorescence band shapes with td-dft, *Journal of Chemical Theory and Computation* 9 (6) (2013) 2749–2760, pMID: 26583866. arXiv:<https://doi.org/10.1021/ct4000795>, doi:10.1021/ct4000795. URL <https://doi.org/10.1021/ct4000795>
- [9] E. Kim, Y. Lee, S. Lee, S. B. Park, Discovery, Understanding, and Bioapplication of Organic Fluorophore: A Case Study with an Indolizine-Based Novel Fluorophore, *Seoul-Fluor. Accounts of Chemical Research* 48 (3) (2015) 538–547. doi:10.1021/ar500370v.
- [10] S. R. Ibrahim, G. A. Mohamed, Marine Pyridoacridine Alkaloids: Biosynthesis and Biological Activities, *Chemistry and Biodiversity* 13 (1) (2016) 37–47. doi:10.1002/cbdv.201400434.
- [11] S. R. Ibrahim, G. A. Mohamed, Pyridoacridine alkaloids from deep-water marine organisms: Structural elucidation, *Bulletin of Faculty of Pharmacy, Cairo University* 54 (2) (2016) 107–135. doi:10.1016/j.bfopcu.2016.08.003.
- [12] A. R. Carroll, P. J. Scheuer, Kuanoniamines A, B, C, and D: Pentacyclic Alkaloids from a Tunicate and Its Prosobranch Mollusk Predator *Chelynotus semperi*, *Journal of Organic Chemistry* 55 (14) (1990) 4426–4431. doi:10.1021/jo00301a040.
- [13] G. P. Gunawardana, F. E. Koehn, A. Y. Lee, J. Clardy, H. Yin He, D. J. Faulkner, Pyridoacridine Alkaloids from Deep-Water Marine Sponges of the Family Pachastrellidae: Structure Revision of Dercitin and Related Compounds and Correlation with the Kuanoniamines, *Journal of Organic Chemistry* 57 (5) (1992) 1523–1526. doi:10.1021/jo00031a035.
- [14] D. Skyler, C. H. Heathcock, The pyridoacridine family tree: A useful scheme for designing synthesis and predicting undiscovered natural products, *Journal of Natural Products* 65 (11) (2002) 1573–1581. doi:10.1021/np020016y.
- [15] J. A. Joule, M. Álvarez, Pyridoacridines in the 21st Century, *European Journal of Organic Chemistry* 2019 (31–32) (2019) 5043–5072. doi:10.1002/ejoc.201900401.
- [16] J. B. Li, H. W. Liu, T. Fu, R. Wang, X. B. Zhang, W. Tan, Recent Progress in Small-Molecule Near-IR Probes for Bioimaging, *Trends in Chemistry* 1 (2) (2019) 224–234. doi:10.1016/j.trechm.2019.03.002.
- [17] M. J. Frisch, G. W. Trucks, H. B. Schlegel, G. E. Scuseria, M. A. Robb, J. R. Cheeseman, G. Scalmani, V. Barone, G. A. Petersson, H. Nakatsuji, X. Li, M. Caricato, A. V. Marenich, J. Bloino, B. G. Janesko, R. Gomperts, B. Mennucci, H. P. Hratchian, J. V. Ortiz, A. F. Izmaylov, J. L. Sonnenberg, D. Williams-Young, F. Ding, F. Lipparini, F. Egidi, J. Goings, B. Peng, A. Petrone, T. Henderson, D. Ranasinghe, V. G. Zakrzewski, J. Gao, N. Rega, G. Zheng, W. Liang, M. Hada, M. Ehara, K. Toyota, R. Fukuda, J. Hasegawa, M. Ishida, T. Nakajima, Y. Honda, O. Kitao, H. Nakai, T. Vreven, K. Throssell, J. A. Montgomery, Jr., J. E. Peralta, F. Ogliaro, M. J. Bearpark, J. J. Heyd, E. N. Brothers, K. N. Kudin, V. N. Staroverov, T. A. Keith, R. Kobayashi, J. Normand, K. Raghavachari, A. P. Rendell, J. C. Burant, S. S. Iyengar, J. Tomasi, M. Cossi, J. M. Millam, M. Klene, C. Adamo, R. Cammi, J. W. Ochterski, R. L. Martin, K. Morokuma, O. Farkas, J. B. Foresman, D. J. Fox, *Gaussian<sup>16</sup> Revision C.01*, gaussian Inc. Wallingford CT (2016).
- [18] A. D. Becke, A new mixing of Hartree-Fock and local density-functional theories, *The Journal of Chemical Physics* 98 (2) (1993) 1372–1377. doi:10.1063/1.464304.
- [19] C. Lee, C. Hill, N. Carolina, Development of the Colle-Salvetti correlation-energy formula into a functional of the electron density, *Chemical Physics Letters* 162 (3) (1989) 165–169. arXiv:[PhysRevA.38.3098](https://arxiv.org/abs/PhysRevA.38.3098), doi:10.1016/0009-2614(89)85118-8.
- [20] S. H. Vosko, L. Wilk, M. Nusair, Accurate spin-dependent electron liquid correlation energies for local spin density calculations: a critical analysis, *Canadian Journal of Physics* 58 (8) (1980) 1200–1211. doi:10.1139/p80-159.
- [21] T. Yanai, D. P. Tew, N. C. Handy, A new hybrid exchange–correlation functional using the coulomb-attenuating method (cam-b3lyp), *Chemical Physics Letters* 393 (1) (2004) 51–57. doi:<https://doi.org/10.1016/j.cplett.2004.06.011>. URL <https://www.sciencedirect.com/science/article/pii/S0009261404000000>
- [22] C. Adamo, V. Barone, Toward reliable density functional methods without adjustable parameters: The PBE0 model, *Journal of Chemical Physics* 110 (13) (1999) 6158–6170. doi:10.1063/1.478522.
- [23] V. Barone, M. Cossi, Quantum calculation of molecular energies and en-

- ergy gradients in solution by a conductor solvent model, *Journal of Physical Chemistry A* 102 (11) (1998) 1995–2001. doi:10.1021/jp9716997.
- [24] M. Cossi, N. Rega, G. Scalmani, V. Barone, Energies, structures, and electronic properties of molecules in solution with the C-PCM solvation model, *Journal of Computational Chemistry* 24 (6) (2003) 669–681. doi:10.1002/jcc.10189.
- [25] M. Caricato, B. Mennucci, J. Tomasi, F. Ingrosso, R. Cammi, S. Corni, G. Scalmani, Formation and relaxation of excited states in solution: a new time dependent polarizable continuum model based on time dependent density functional theory, *The Journal of chemical physics* 124 (12) (2006) 124520. doi:10.1063/1.2183309.  
URL <https://doi.org/10.1063/1.2183309>
- [26] F. J. Avila Ferrer, J. Cerezo, E. Stendardo, R. Improta, F. Santoro, Insights for an accurate comparison of computational data to experimental absorption and emission spectra: Beyond the vertical transition approximation, *Journal of Chemical Theory and Computation* 9 (4) (2013) 2072–2082, pMID: 26583553. arXiv:<https://doi.org/10.1021/ct301107m>, doi:10.1021/ct301107m.  
URL <https://doi.org/10.1021/ct301107m>
- [27] D. Jacquemin, T. L. Bahers, C. Adamo, I. Ciofini, What is the "best" atomic charge model to describe through-space charge-transfer excitations?, *Physical Chemistry Chemical Physics* 14 (16) (2012) 5383–5388. doi:10.1039/c2cp40261k.
- [28] L. P. Hammett, The Effect of Structure upon the Reactions of Organic Compounds. Benzene Derivatives, *Journal of the American Chemical Society* 59 (1) (1937) 96–103. doi:10.1021/ja01280a022.
- [29] G. S. Remya, C. H. Suresh, Quantification and classification of substituent effects in organic chemistry: A theoretical molecular electrostatic potential study, *Physical Chemistry Chemical Physics* 18 (30) (2016) 20615–20626. doi:10.1039/c6cp02936a.
- [30] C. Hansch, A. Leo, R. W. Taft, A Survey of Hammett Substituent Constants and Resonance and Field Parameters, *Chemical Reviews* 91 (2) (1991) 165–195. doi:10.1021/cr00002a004.
- [31] D. Cheshmedzhieva, P. Ivanova, S. Stoyanov, D. Tasheva, M. Dimitrova, I. Ivanov, S. Ilieva, Experimental and theoretical study on the absorption and fluorescence properties of substituted aryl hydrazones of 1,8-naphthalimide, *Physical Chemistry Chemical Physics* 13 (41) (2011) 18530–18538. doi:10.1039/c1cp21756a.